Structural, Electrical and Magnetic Properties of FeO added GdBaCuO Superconductors

Hasan Ağıl[1,✉], Nurcan Akduran[2]

ABSTRACT. In this study, the effects of FeO addition (0, 1, 2, 3, 4, 5, 10 and 20 wt %) on the structural, electrical and magnetic properties of GdBaCuO-123 (Gd-123) superconductor prepared by the conventional solid state method were investigated. The phase analysis and the lattice parameters of the materials were analyzed by X-ray diffraction (XRD) method. The critical temperatures (T_c) of the samples were determined from the resistance measurements by the standard four-point probe method. From these measurements, superconducting behaviour was observed for the addition of FeO up to 5 wt %. On the other hand, semiconducting behaviour was observed for higher FeO additions (10 and 20 wt %). The activation energies (U_0) were also evaluated by using the thermally-assisted-flux-flow (TAFF) model from the resistance measurements of the samples. It was observed that the activation energy of the samples decreased with the increase of the amount of FeO. The magnetic measurements of the samples (M-H) were carried out at 20 K with the Quantum Design PPMS system. Critical current densities (J_c) were calculated from the width of the M-H curves by using the Bean critical state model. According to the obtained results, the highest current carrying capacity belongs to 1 wt % added sample and has 1.2×10^4 A/cm^2 value at 20 K and 0 T. It was also found that all samples were still carrying high currents even in high fields.

Keywords: GdBaCuO superconductor; FeO addition; Flux pinning; Critical current density.

INTRODUCTION

The discovery of copper oxide based high temperature superconductors by Bednorz and Müller in 1986[1] has created worldwide interest in these materials. Many researchers have focused on investing the superconducting properties of high temperature superconductor improving the micro structural and crystallographic quality of the bulk samples during the last years.[2-4] REBCO type superconductors (RE: Rare Earth Elements, B: Ba, C: Cu) attract great attention due to their high potential in basic research and large-scale applications.[5-7] Deviations from stoichiometry significantly change the characteristics of high-temperature superconductors. Some additives eliminate superconductivity and can affect the CuO$_2$ plane, which is responsible for superconductivity for high temperature superconductors. Studies show that additions to REBCO compounds act as pinning centers, creating imperfections in the superconductor.[8] In this way vortex movement can be prevented. Transport critical current density (J_c) is an important parameter of superconductors for possible applications. J_c strongly depends on the distribution and size of flux pinning centers. It is known that high critical current density in REBCO type superconductors requires effective vortex pinning. Because of this feature, it is possible to improve the pinning mechanism with different non-superconducting chemical impurity addition. These impurities try as flux pinning centers guides to the strengthening of J_c. It has been reported that iron addition is effective in improving electrical and magnetic properties of the superconducting oxides.[9-11] Various studies have been carried out to substitute Fe in Cu sites to improve the superconductivity properties of REBa$_2$Cu$_3$O$_7$.[12-13]

✉ Corresponding author.
  E-mail address: hasanagil@hakkari.edu.tr (H. Ağıl)

[1] Department of Material Science and Engineering, Faculty of Engineering, Hakkari University, Hakkari, Turkey

[2] Technology Department, Sarayköy Nuclear Research and Training Centre, Turkish Atomic Energy Authority, Ankara, Turkey

High temperature bulk superconductors are frequently used in applications such as magnetic levitation and electric generators. For this reason, many research groups around the world have been investigating to improve and investigate the structural, electrical and magnetic properties of these materials.[14-15]

Superconductors, as known, exhibit diamagnetic properties below the critical temperature. However, the discovery of iron-based superconductors in recent years is quite interesting.[16] Because, as is known, iron is a ferromagnetic material. Since a material containing a ferromagnetic element exhibits superconducting properties, researchers show great interest in such materials. Therefore, in this study, we aimed to investigate the effects of iron addition on GdBaCuO superconductor. It acts as flux pinning centers to enhance the transport critical current density. A systematic work on crystal structure, electrical and magnetic properties of a set of samples (x = 0 - 20 wt %) are reported.

MATERIALS AND METHODS

The polycrystalline samples produced for this study were prepared by the solid-state reaction route. Gd_2O_3, $BaCO_3$ and CuO were used as starting powders and were weighed at nominal stoichiometric ratios according to the chemical formula $GdBa_2Cu_3O$. The purity of the raw materials was $\geq$ 99.9%. The starting powders were mixed and ground by using an agate mortar and pestle. Samples were calcined at 965 °C for 48 h in air atmosphere to remove carbonate residues and this process was repeated twice by intermediate grinding. After this process, the samples were synthesized for 48 h to form $GdBa_2Cu_3O_7$ at 965 °C and annealed at 500 °C for 36 h in oxygen atmosphere. After annealing, the samples were cooled in the furnace to room temperature. After the production of the pure material was completed, different amounts (x = 0, 1, 2, 3, 4, 5, 10 and 20 wt. %) of FeO were added to the $GdBa_2Cu_3O_7$ superconductor. Finally, all the materials were pelletized in disc form under a pressure of 1050 MPa. The thickness and diameter of the materials are 0.15 and 1 cm, respectively.

The GBCO + x(FeO) samples were sintered at temperatures ranging 965 $\pm$ 5 °C for 24 h in oxygen medium and cooled to 520 °C in 8 h. The sintered samples were annealed at 520 °C in the flowing oxygen for 24 h to provide complete oxygenation. After annealing, once again samples cooled to room temperature in the furnace. Samples prepared with different FeO addition with x = 0, 1, 2, 3, 4, 5, 10 and 20 % in GdBaCuO will then be denoted as F0, F1, F2, F3, F4, F5, F6 and F7, respectively.

The crystal structures of the samples were characterized by the powder X-ray diffraction technique with using Cu-K$_\alpha$ radiation (λ = 1.5406 Å) with Bruker Powder X-ray diffractometer. Electrical-resistivity measurements of the samples were performed by the four point resistivity measurements within 77 - 300 K.

The magnetic measurements of the samples (M-H) were carried out at 20 K with the Quantum Design PPMS system. Critical current densities (J_c) were calculated from the width of the M-H curves by using the Bean critical state model:

$$J_c = \frac{20\,\Delta M}{\left(a\left(1 - \frac{a}{3b}\right)\right)} \qquad (1)$$

Here $\Delta M = M^+ - M^-$ is the width of the hysteresis loop, a and b are width and length of the sample, respectively. The activation energies (U_0) were also evaluated by using the thermally-assisted-flux-flow (TAFF) model from the resistance measurements of the samples.
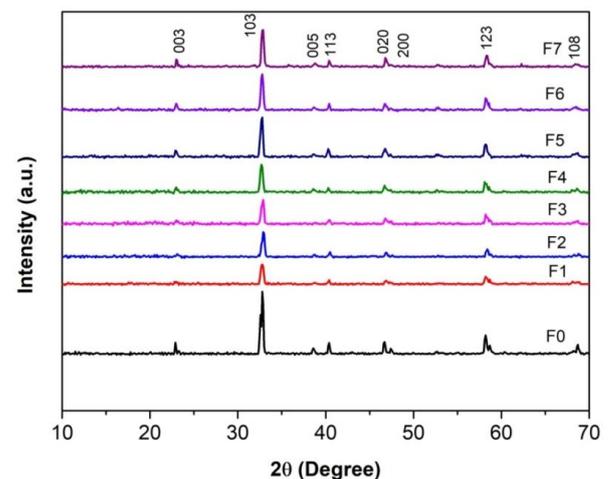

Fig. 1: X-ray diffraction patterns for all samples.

RESULTS AND DISCUSSION

As X-ray diffraction patterns were determined using Bruker AXS D8 powder diffractometer (Cu-K$_\alpha$ radiation, λ = 1.5406 Å). The XRD patterns of all samples are shown in Fig. 1. It is clearly seen from the XRD analysis that the main phase is Gd-123 in all samples. Considering that Gd-123 phases have orthorhombic symmetry, lattice parameters were

calculated and shown in Table 1. These calculations were made using data from XRD measurements.

Table 1. Lattice parameters of all samples.

Sample	a (Å)	b (Å)	c (Å)	V (Å^3)
F0	3.839	3.893	11.675	174.51
F1	3.830	3.871	11.748	174.20
F2	3.836	3.873	11.651	173.14
F3	3.842	3.887	11.662	174.21
F4	3.857	3.890	11.687	175.42
F5	3.857	3.882	11.700	175.23
F6	3.829	3.885	11.711	174.26
F7	3.828	3.880	11.722	174.11

Table 2: Critical temperatures of pure and FeO added Gd-123 superconductors.

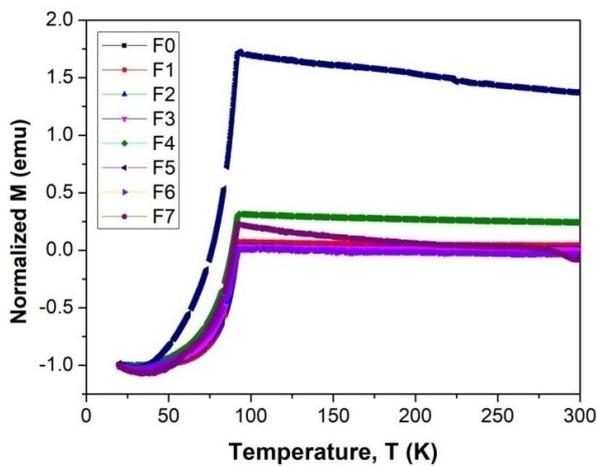| Samples	$T_{c,onset}$ (K)
F0	93.1
F1	92.4
F2	92.4
F3	92.1
F4	92.1
F5	92.1
F6	92
F7	92

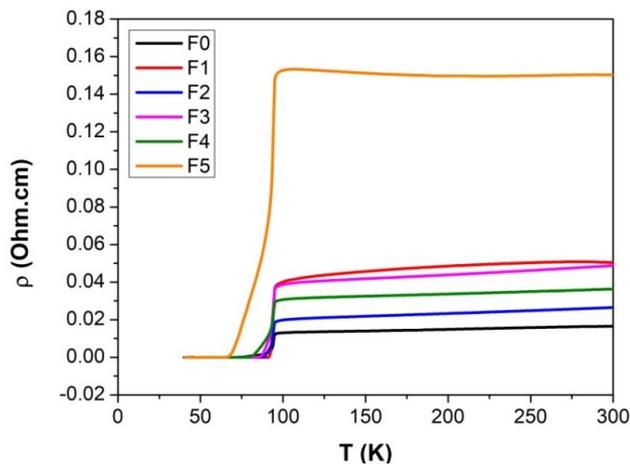**Fig. 2:** The normalized magnetic moments of all samples as a function of temperature.

Fig. 3: Temperature dependence of resistivity in F0 - F5 samples.

The critical temperatures of the samples were determined by both resistivity (ρ-T) and magnetization (M-T) measurements. Firstly, the obtained results from the magnetization measurements will be discussed. Fig. 2 shows the normalized magnetic moments of all samples as a function of temperature. As can be seen from the graph, the transition of all samples from the normal state to the superconducting state takes place in a sharp but a wide range. In addition, the onset critical temperatures of the samples are slightly reduced by increasing the amount of FeO. Table 2 shows the onset critical temperature values ($T_{c,onset}$) determined from the magnetization measurements of all samples. It is thought that the reason for this is that the Fe^{2+} ions are replaced by Gd^{3+} or Ba^{2+} ions in the sintering process, which degrades the superconducting transition temperatures of Gd-123 samples.
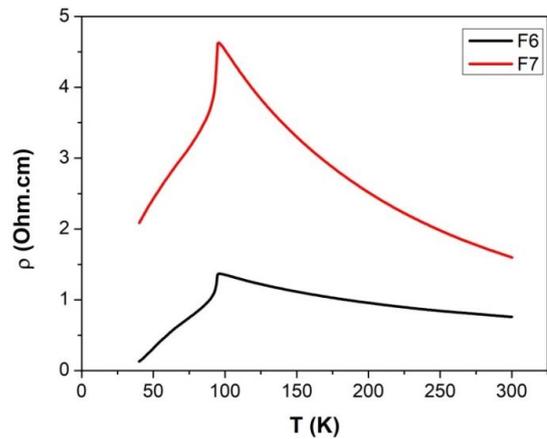

Fig. 4: Temperature dependence of resistivity in F6 and F7 samples.

Fig. 3 shows the resistivity curves as a function of temperature for the F0 - F5 samples. As seen in the graph, diamagnetic behavior, which is characteristic of superconductors, is exhibited in these materials. On the other hand, as shown in Fig. 4, when the resistivity-temperature curves of F6 and F7 samples are examined, it can be seen that they exhibit semiconductor behavior. This behavior occurs in the resistivity measurements when there is no such behavior in magnetic measurements for these materials. The susceptibility, magnetization and dc resistivity measurements are generally used to determine the transition temperature of superconducting materials. In the susceptibility and magnetization measurements, the bulk sample is exposed directly to the magnetic field and the transition temperature is determined from the response of this field. However, the following parameters are important

to determine the transition temperature from the resistivity measurements:

  i.   The geometry of the sample being contacted
  ii.   The size and thickness of the sample
  iii. The contact resistance
  iv.   Most importantly, the sample is pressed into a single-axis pellet in the preparation process.

Table 3 gives the critical temperature values from the resistance measurements of all samples. Compared to pure sample, critical temperatures of FeO added samples change very little and the critical temperature values never change with the increase of FeO amount.

Table 3. Critical temperatures of pure and FeO added Gd-123 superconductors.

Samples	$T_{c,onset}$ (K)
F0	95.8
F1	95.2
F2	95.2
F3	95.2
F4	95.2
F5	95.2
F6	-
F7	-

Carrier concentration is calculated using the following well-known equation:[17]

$$\frac{T_c}{T_c^{max}} = 1 - 82.6(p - 0.16)^2 \tag{2}$$

The change in carrier concentration with $T_{c,zero}$ is given in Fig. 5. The results clearly show that $T_{c,zero}$ is more sensitive to changes in FeO concentration. Decreasing the $T_{c,zero}$ values may be due to the weak link between the Gd-123 grains, the deterioration of the structure and the lattice defect of the additive.
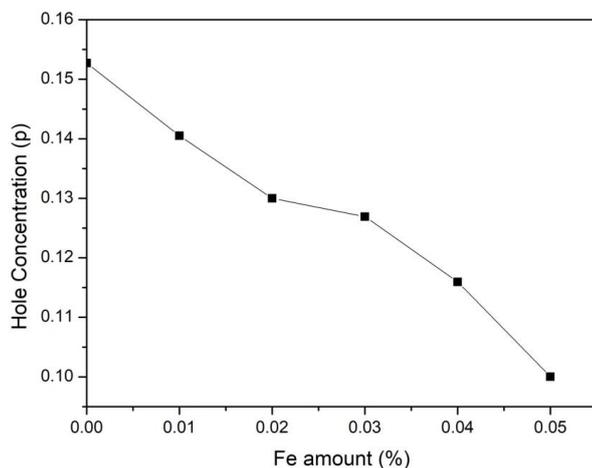

Fig. 5: Variation of the hole-carrier concentration vs. Fe-amount.

The resistivity in the TAFF regime can be written as $\rho = \rho_0(B,T) \exp(-U_0/k_{BT})$, so the activation energy can be obtained by plotting $\ln(\rho/\rho_0)$ against T^{-1}. Fig. 6 shows the Arrhenius graph of the activation energy of the samples given by the slope of the low-resistance linear region.
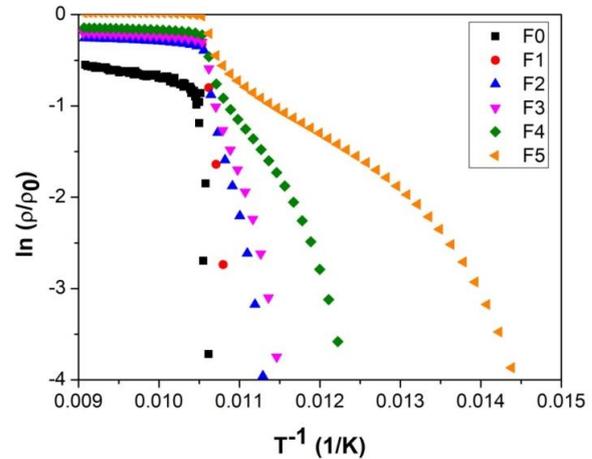

Fig. 6: Arrhenius plots of the resistive transition of the samples.

For each sample, the obtained activation energy is plotted as a function of the addition amount, as shown in Fig. 7, in order to determine the dependence of the TAFF activation energy (U_0) on the addition amount. It is clear that the activation energy has decreased considerably with the increase of the addition amount.
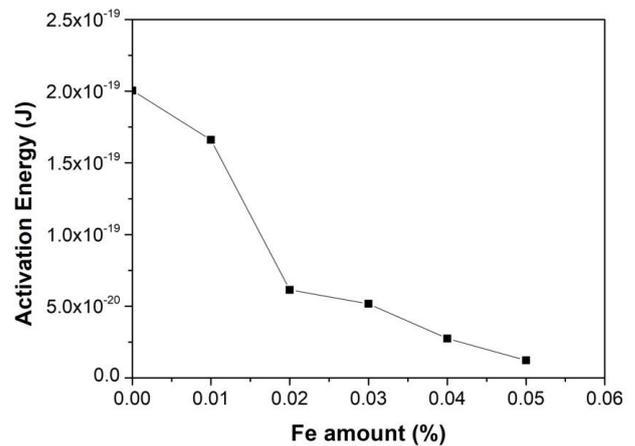

Fig. 7: U_0 dependence on FeO addition amount for samples.

Fig. 8 shows the magnetic field dependence of the J_c determined from the width of *M-H* curves using the Bean critical state model.[18] When F1 and F2 samples are compared with other samples, it is seen that they carry higher current in both low and high magnetic field. According to the obtained results, the highest current carrying capacity belongs to 1 wt % added sample and has 1.2×10^4 A/cm^2 value at 20 K and 0 T.
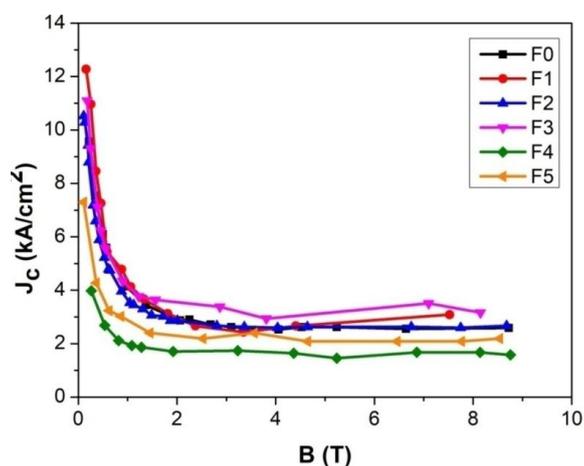
Fig. 8: The magnetic field dependence of J_c for all samples.

In Table 4, the critical current density values are given at 20 K and 0 and 8 T for all samples.

Table 4. Critical current density values for all samples.

Samples	J_c (kA/cm^2)	
	Self-field	8 T
F0	9.5	2.5
F1	12.3	3.1
F2	10.5	2.7
F3	11.1	3.2
F4	3.9	1.5
F5	7.3	2.2
F6	-	-
F7	-	-

Based on these results, it was demonstrated that the improvement of critical current density up to x < 3. For this reason, we can say that the optimum amount of adding for FeO addition to Gd-123 superconductor is x < 3.

CONCLUSION

In this study, the various addition levels of FeO to Gd-123 superconductor were successfully accomplished by the conventional solid state sintering method. It has been observed from both the magnetization and resistance measurements that the critical temperatures of the samples change very little with the increase in the amount of addition. Semiconducting behavior was observed in the resistance measurements of F6 and F7 samples and it was interpreted that this behavior may depend on many parameters. The activation energies of the samples were determined by using the thermally assisted flux flow (TAFF) regime and the activation energies of the samples decreased with increasing the amount of additive. It has been observed that the critical current densities of the samples increase with FeO addition up to x < 3. Hence, as a concluding remark, it could be said that the optimum amount of addition is x < 3.

REFERENCES

1. Bednorz JG, Müller KA. Possible high Tc superconductivity in the Ba-La-Cu-O system. Z. Phys. B 1986;64:189-193.

2. Pang P, Liu W, Ren X, Lu Q, Yang S, Jing H, Zhou, X. Temperature characteristics of bulk YBCO exposed to high frequency fluctuant magnetic field in high-Tc superconducting maglev system. Physica C 2020;572:1353616.

3. Mukherjee P, Rao VV. Design and development of high temperature superconducting magnetic energy storage for power applications - A review. Physica C 2019;563:67-73.

4. Kong W, Kong I, Kechik MMA, Shukor RA. Effect of graphene addition on the transport critical current density of bulk (Tl$_{0.85}$Cr$_{0.15}$) Sr$_2$CaCu$_2$O$_{7-\delta}$ superconductor. Mater. Today 2018;5:3176-3184.

5. Kang R, Uglietti D, Song Y. Modelling quench of a 50 kA REBCO conductor with soldered-twisted-stacked-tape-cable strands. Cryogen. 2020;106:103037.

6. Zheng T, Wang W, Liu L, Liu S, Li Y. Superconducting properties of binary rare-earth HoREBCO thin films prepared by pulsed layer deposition. Ceram. Int. 2019;45:13193-13197.

7. Sugino M, Mizuno K, Tanaka M, Ogata M. Development of a REBCO HTS magnet for Maglev - repeated bending tests of HTS pancake coils. Physica C 2018;544:13-17.

8. Smith DA. Interaction of dislocations with grain boundaries. J. Phys. Colloq. 1982;43:225-237.

9. Stewart GR. Superconductivity in iron compounds. Rev. Mod. Phys. 2011;83:1589-1652.

10. Masnita MJ, Shukor RA. Iron sulfide effects on AC susceptibility and electrical properties of Bi$_{1.6}$Pb$_{0.4}$Sr$_2$CaCu$_2$O$_8$ superconductor. Results Phys. 2020;17:103177.

11. Paglione J, Greene RL. High-temperature superconductivity in iron-based materials. Nature Phys. 2010;6:645-658.

12. Gonsalves SH, Monteiro JFHL, Da Silva Leal AC, de Andrade AVC, de Souza GB, Siqueira EC, Serbena FC, Jurelo AR. Fe-Doping effect on the Bi$_3$Ni superconductor microstructure. Mater. Res. 2017;20:601-606.

13. Ben Salem MK, Slimani Y, Hannachi E, Ben Azzouz F, Ben Salem M. Bi-based superconductors prepared with addition of CoFe2O4 for the design of a magnetic probe. Cryogen. 2018;89:53-57.

14. Güner SB, Abdioğlu M, Öztürk K, Çelik Ş. The comparison of levitation and lateral force of bulk and cut-pasted bulk GdBCO samples at different temperatures. J. Alloys Comp. 2020;822:153637.

15. Zhou DF, Xu K, Hara S, Li BZ, Izumi M. NiFe alloy particles doping effect of Gd-Ba-Cu-O bulks processed by a new cold-seeding technology. Transact. Nonferr. Metals Soc. China 2013;23:2042-2046.

16. Kamihara Y, Hiramatsu H, Hirano M, Kawamura R, Yanagi H, Kamiya T, Hosono H. Iron-based layered superconductor: LaOFeP. J. Am. Chem. Soc. 2006;128:10012-10013.

17. Presland MR, Tallon JL, Buckley RG, Liu RS, Flower NE. General trends in oxygen stoichiometry effects on Tc in Bi and

Tl superconductors. Physica C 1991;176:95-105.

18. Bean CP. Magnetization of high-field superconductors. Rev. Mod. Phys. 1964;36:31-39.